Histol Histopathol (2016) 31: 867-877

http://www.hh.um.es

Histology and Histopathology

From Cell Biology to Tissue Engineering

Histological and biochemical characteristics of the rabbit anterior cruciate ligament in comparison to potential autografts

Mariann Hoyer[1,2], Carola Meier[3], Benjamin Kohl[3], Anke Lohan[4], Maria Kokozidou[5] and Gundula Schulze-Tanzil[5]

[1]Department of Bioanalytics, Technical University, Berlin, [2]Central Laboratory, DRK Manniske-Hospital Bad Frankenhausen, Bad Frankenhausen/Kyffhäuser, [3]Department of Orthopaedic, Trauma and Reconstructive Surgery, Charité-Universitätsmedizin Berlin, Campus Benjamin Franklin, Berlin, [4]Forschungseinrichtung für Experimentelle Medizin, Charité-Universitätsmedizin Berlin, Campus Benjamin Franklin, Berlin and [5]Department of Anatomy, Paracelsus Medical University, Nuremberg, Germany

Summary. Tissue engineering of an anterior cruciate ligament (ACL) implant with ACL cells requires detailed analysis of the tissue characteristics that should be mimicked. Therefore, we studied the histological and biochemical properties of rabbit derived ACLs in comparison to other knee-associated tendons that are used as autografts in men.

Rabbit derived ACLs and *Musculus (M.) semimembranosus, M. semitendinosus* tendons and patellar ligaments were explanted from adult New Zealand white rabbits and analyzed histologically for tissue organization (e.g. cellularity, nuclear shapes, elastic fibers), total collagen and sulfated glycosamino-glycan (sGAG) contents. Gene expression analysis was performed for the main extracellular matrix (ECM) components type I collagen, decorin and the glycoprotein tenomodulin.

The ACLs had an average dimension of 1.39x0.39x0.1 cm *in situ*. They were characterized by high sGAG content in comparison to the other tendons/ligaments, whereas the total collagen content did not differ. ACLs possessed higher cellularity and lower feret diameter of the cell nuclei compared with the investigated rabbit-derived tendons. In ACLs long elastic fibers were observed. Concerning the gene expression level, lower transcription of tenomodulin was detected in the ACL compared with the other tendons, without significant difference in the decorin gene expression. The *M. semitendinosus* tendon had a significantly higher type I collagen expression than the ACL and the other investigated tendons.

This phenotypical characterization of the lapine ACL presented in this study provides some key standards to evaluate tissue engineered ACL constructs to be tested in the rabbit model.

Key words: Anterior cruciate ligament, Patellar ligament, Autograft, New Zealand White Rabbit, TNMD

Offprint requests to: Gundula Schulze-Tanzil, VMD, Institute of Anatomy, Paracelsus Medical University, Salzburg and Nuremberg, Germany, Prof. Ernst Nathan Str. 1, 90419 Nuremberg, Germany. e-mail: gundula.schulze@pmu.ac.at or gundula.schulze-tanzil@klinikum-nuernberg.de

DOI: 10.14670/HH-11-723

Introduction

ACL rupture and adequate ACL reconstruction remain major issues in orthopedics. The rabbit is a

Abbreviations. ACL, anterior cruciate ligament; COL1A1, gene coding for type I collagen; DCN, gene coding for decorin; DMEM, Dulbecco's Modified Eagle's; DMMB, dimethyl methylene blue; ECM, extracellular matrix; FCS, fetal calf serum; GAPDH, glyceraldehyde-3-phosphate dehydrogenase; HE, hematoxylin and eosin staining; l, lapine; M, musculus; PBS, phosphate buffered saline; PFA, paraformaldehyde; RT, room temperature; SCX, gene coding scleraxis; SD, standard deviation; sGAG, sulfated glycosaminoglycans; TBS, TRIS buffered saline; TNC, gene coding tenascin C; TNMD, gene coding for tenomodulin

commonly used model to study various novel approaches of ACL reconstruction (Kawai et al., 2010; Lee et al., 2012; Bachy et al., 2013; Shen et al., 2014). The mode of biomechanical failure during experimental rupturing of human and lapine ACLs was very similar (Azangwe et al., 2001). However, the extent of result transferability gained in the rabbit model as opposed to human conditions remains unclear (Azangwe et al., 2001). In the end, histomorphological and biochemical markers are required to monitor the healing process in response to ACL graft implantation. Furthermore, the characterization of the ACL phenotype is an important quality control measure with regard to cell-based ACL construct generation based on tissue engineering methods (Petrigliano et al., 2006; Hoyer et al., 2014, 2015; Hahner, 2015). The ACL is an intra-articular ligament localized between the fibrous and synovial layer of the joint capsule. It is therefore, in contrast to other periarticular ligaments, separated only by the thin synovial membrane from the synovial fluid and immediately neighbored to the Hoffa fat pad and connected to it by a synovial fold (Benedetto and Klima, 1986). The patellar ligament and the *M. semimembranosus* and *M. semitendinosus* tendons which belong to the so called "hamstring" tendons (including *M. semimembranosus, M. semiten-dinosus* and *M. biceps femoris*) are usually used in humans as autografts for ACL reconstruction (Blickenstaff et al., 1997; Marumo et al., 2005; Chambat, 2013) and were hence included in this study. Donor site morbidity has been described previously in response to harvesting hamstring tendons and patellar ligaments as autografts. The hamstring muscles protect the ACL by providing biomechanical joint stability (Biscarini et al., 2013). After grafting, *M. semiten-dinosus* muscles developed a smaller cross-sectional area (Eriksson et al., 2001). The revascularization of grafts for ACL reconstruction is also a challenging issue (Tohyama et al., 2009).

Tendons and ligaments are generally poorly supplied with blood vessels. The ACL receives supply from the local environment, the covering synovial membrane and infrapatellar fat pad and is therefore like other ligaments and tendons classified as bradytrophic tissue (Arnoczky, 1985). The vascularization of tendons varies depending on the local environment (Fenwick et al., 2002). Meanwhile, it is known that the biochemical composition differs between tendon and ligaments (Amiel et al., 1986; Kato et al., 2015). Some comparative analyses of the expression profile of ligaments and ligament-derived cells, including the ACL and patellar ligaments but not the hamstring tendons, have already been previously undertaken, which indicated distinct differences (Amiel et al., 1984; Lo et al., 2004; Kato et al., 2015). However, these studies remained limited to selected parameters. Kato and colleagues e.g. analyzed enzymes involved in collagen maturation in cultured ligament fibroblasts of the ACL, collateral and patellar ligaments (Kato et al., 2015).

Materials and methods

Explantation of tendon and ligaments

Tendons/ligaments were harvested *post mortem* from skeletally mature New Zewland White rabbits with a body weight of 2.8-3.5 kg (12-15 months old). The dimensions of the 13 rabbit ACLs were measured *in situ* before and three of them also after explantation. 4 patellar ligaments, 7 *M. semimembranosus* and 6 *M. semitendinosus* tendons were explanted for analyses. Additionally, cartilage slices were harvested from the patellar groove, femur condyles and tibia plateau for RNA isolation (n=5) as a control for quantitative total collagen content and soluble glycosaminoglycan (sGAG) analysis. Three human ACLs were included in this study for comparison (gene expression analysis).

Sampling of human ACL was approved by the local ethics committee of the Charité-Universitätsmedizin Berlin (intern number: EA4033/08). Human ACLs were harvested during knee joint replacement surgeries (5 female and 2 male patients with an age between 46-82 years and a mean age of 71.85 years).

Histological staining procedures

The ACL was explanted *en bloc* with its enthesis and the subenthesial bone region. It was fixed for 3 days with a 4% paraformaldehyde (PFA) ready to use solution (USB, USA) and stored at 4°C. Subsequently, samples were decalcified for 3-4 weeks in 100 g/l EDTA solution (pH 8.0, Merck, Darmstadt, Germany) and dehydrated before embedding in paraffin wax (Merck, Germany) and preparing 5 μm sections. The other tendons were treated in a similar manner without decalcification. Sections were stained using hematoxylin and eosin (HE) for cell characterization.

Sections were incubated for 6 min in Harry's hematoxylin (Sigma-Aldrich), before rinsing in water and counterstaining for 4 min with eosin (Carl Roth GmbH, Karlsruhe, Germany). For detection and localization of sGAGs, safranin O (SO) (Merck) staining with fast green (Sigma-Aldrich) counterstaining or alcian blue (AB) stainings were used. To perform AB staining the sections were incubated for 3 min in 1% acetic acid and then incubated for 30 min in 1% AB (Carl Roth GmbH). Subsequently, after rinsing in 3% acetic acid and 2 min washing in A. dest., cell nuclei were counterstained in nuclear fast red aluminium sulphate solution (Carl Roth GmbH) for 5 min.

Elastic fibers were detected by resorcin-fuchsin staining. Paraffin sections were stained in Weigert's resorcin-fuchsin (Waldeck GmbH, Münster, Germany) for 5 min. Then, differentiation in hydrochloric acid/ethanol for 1 min followed. After washing with tap water for 10 min, a washing step in distilled water followed. Nuclear fast red aluminium sulphate solution (Carl Roth GmbH) was used to counterstain the cell

nuclei.

Cell counting and measurement of cell nuclei dimensions

Three HE stained images (magnification 200 fold) of three (*M. semitendinosus, M. semimembranosus* and patellar) or four (ACL) tendon/ligament donors were used to assess whole, round shaped and elongated cell numbers. The area of cell nuclei of twelve separate and randomly selected cells of three images per tendon was measured to calculate the feret nucleus diameter. ImageJ 1.44p with Analysis Plugin (W. Rasband, National Institutes of Health, USA) was used for analysis.

Quantification of ECM components

Samples (ACL and tendon midsubstances without enthesis) were digested using proteinase K (Roche, Mannheim, Germany, 800 ng/ml proteinase K in 50 mM TRIS/HCl, 1 mM EDTA, 0.5% Tween 20 at pH 8.5, all Sigma-Aldrich) for minimum 16 h or until complete digestion at 55°C. After centrifugation for 10 min at 10,000 g, the supernatant was used for sGAG, hydroxyproline and DNA quantification.

After adequate sample dilution the dimethyl methylene blue solution (DMMB, AppliChem, Darmstadt, Germany) was added (40 mM glycine [Sigma-Aldrich], 40 mM NaCl [Carl Roth GmbH] at pH 3 and DMMB [8.9 mM in ethanol]). Chondroitin sulfate (Sigma-Aldrich) was used as standard. The absorption shift was measured at wave length of λ=633 nm to λ=552 nm using a GENios spectral photometer (Tecan, Maennedorf, Switzerland).

In order to assess collagen content via hydroxyproline quantification, lysates were incubated for 24 h with an equal volume of HCl (6 M) at 105°C. Samples were neutralized with NaOH citrate-acetate buffer and subsequently incubated with chloramine T (Merck), perchloric acid (Carl Roth GmbH) and p-dimethylaminobenzaldehyde (J.T.Baker, Deventer, Netherlands) to achieve a red colored product whose light absorption was measured at the wave length of λ=565 nm. A hydroxyproline solution (AppliChem) served as a standard. The measured hydroxyproline concentration was multiplied using the factor 7.1 to calculate the total collagen content (Homicz et al., 2003).

Finally, results of both assays were normalized to the determined cell numbers which were calculated from the DNA content of the lysates measured by the CyQuant NF Assay (Life Technologies, Darmstadt, Germany). This assay was performed as recommended by the manufacturer's protocol based on calf thymus DNA (Sigma-Aldrich) as standard.

Gene expression analysis

RNA isolation

Freshly explanted and snap frozen ACL tissues from New Zealand White Rabbits were crushed using mortar and pestle under liquid nitrogen. The frozen tissue powder was suspended in a suitable volume of Qiazol (Qiagen, Hilden, Germany) and homogenized using an ULTRA-Turrax rotor stator homogenizer (IKA Werke, Staufen, Germany). Then, an adequate volume of 1-bromo-3-chloro-propane was added and the samples were centrifuged at 12,000 g for 15 min. The upper phase was combined with a similar volume of 70% ethanol. The samples were further processed as recommended for the RNeasy Mini Kit (Qiagen) omitting the optional on-column-DNase-digestion-step.

Quality and quantity of the samples total RNA was determined with the Nanodrop ND-1000 spectrophotometer (Peqlab Biotechnologie GmbH, Erlangen, Germany) and Agilent 2100 Bioanalyzer system (Agilent Technologies, USA).

Quantitative real-time PCR

For cDNA synthesis 120 ng of total RNA were reverse transcribed using the QuantiTect Reverse Transcription Kit (Qiagen) according to the supplier manual. 6 ng cDNA were used for each quantitative real-time PCR (qPCR) reaction using TaqMan Gene Expression Assays (Life Technologies) with primer pairs for *COL1A1* (Oc03396073_g1), *DCN* (Hs003703-84_m1), tenomodulin (*TNMD*) (rabbit: Oc033995-05_m1 [synonymous: myodulin] and human: Hs00223332), tenascin C (*TNC*) (Hs01115665_m1),

Table 1. Primers used in this study.

Gene symbol	Species	Gene name	Amplicon length	Assay ID
COL1A1	*O. cuniculus*	collagen type I, alpha 1	70	Oc03396073_g1
DCN	*Homo sapiens*	decorin	77	Hs00370384_m1
GAPDH (LOC100009074)	*O. cuniculus*	glyceraldehyde-3-phosphate dehydrogenase	82	Oc03823402_g1
GAPDH	*Homo sapiens*	glyceraldehyde-3-phosphate dehydrogenase	93	Hs02758991_g1
TNMD (LOC100125994)	*O. cuniculus*	myodulin	146	Oc03399505_m1
TNMD	*Homo sapiens*	tenomodulin	73	Hs00223332_m1
SCXB	*Homo sapiens*	scleraxis homolog B (mouse)	63	Hs03054634_g1
TNC	*Homo sapiens*	tenascin C	61	Hs01115665_m1

scleraxis (*SCX*) (Hs03054634_g1) and the housekeeping gene *GAPDH* (Oc03823402_g1) (see Table 1). qPCR was performed using the real time PCR detector Chromo4 (BioRad, Munich, Germany) thermocycler with the program Opticon Monitor (version 3.1.32, BioRad).

The relative gene expression of the genes of interest (*COL1A1, DCN, TNMD, TNC, SCX*) normalized towards the *GAPDH* expression was calculated for each sample using the ΔΔCT method as described by Livak and Schmittgen (Livak and Schmittgen, 2001).

Statistics

Data were expressed as mean values with standard deviation. Statistics were compiled using GraphPad Prism (version 5.02, GraphPad Software, USA). Statistical significance was set at a p value of ≤0.05. The Grubbs test identified outliers. Data was tested for normal distribution using the Kolmogorov-Smirnov test (α=0.05). For analysis of normally distributed data (qPCR analysis Fig. 5) the unpaired, two-tailed t-test and one way ANOVA with Bonferroni test were used. For data, which did not follow Gauss distribution a one way ANOVA and Dunn post hoc test (e.g. sGAG and collagen contents Fig. 6) was applied.

Results

Anatomical localization of analyzed ligaments and tendons in the rabbit

The patellar ligament and ACL has a comparable localization in the rabbit compared with humans. The lapine ACL is attached to the *area intercondylaris anterior* and the inner part of the lateral femur condyle, in a similar manner to humans. Like in humans the patellar ligament connects the patella with the tibial tuberosity (*tuberositas tibiae*). However, the anatomical localization and macroscopical morphology of the *M. semitendinosus* and *M. semimembranosus* tendons differs substantially compared with human conditions (Fig. 1A-C). The *M. semitendinosus* tendon is attached to the medial part of the tibial tuberosity and sends a branch joining the Achilles tendon. In contrast to humans, in the rabbit it originates from the first tail vertebrae and with a second head from the ischial tuberosity (*tuber ischiadicum*). The *M. semimembranosus*, which originates from the pubic symphysis and its tendon, is attached to the patellar ligament. The

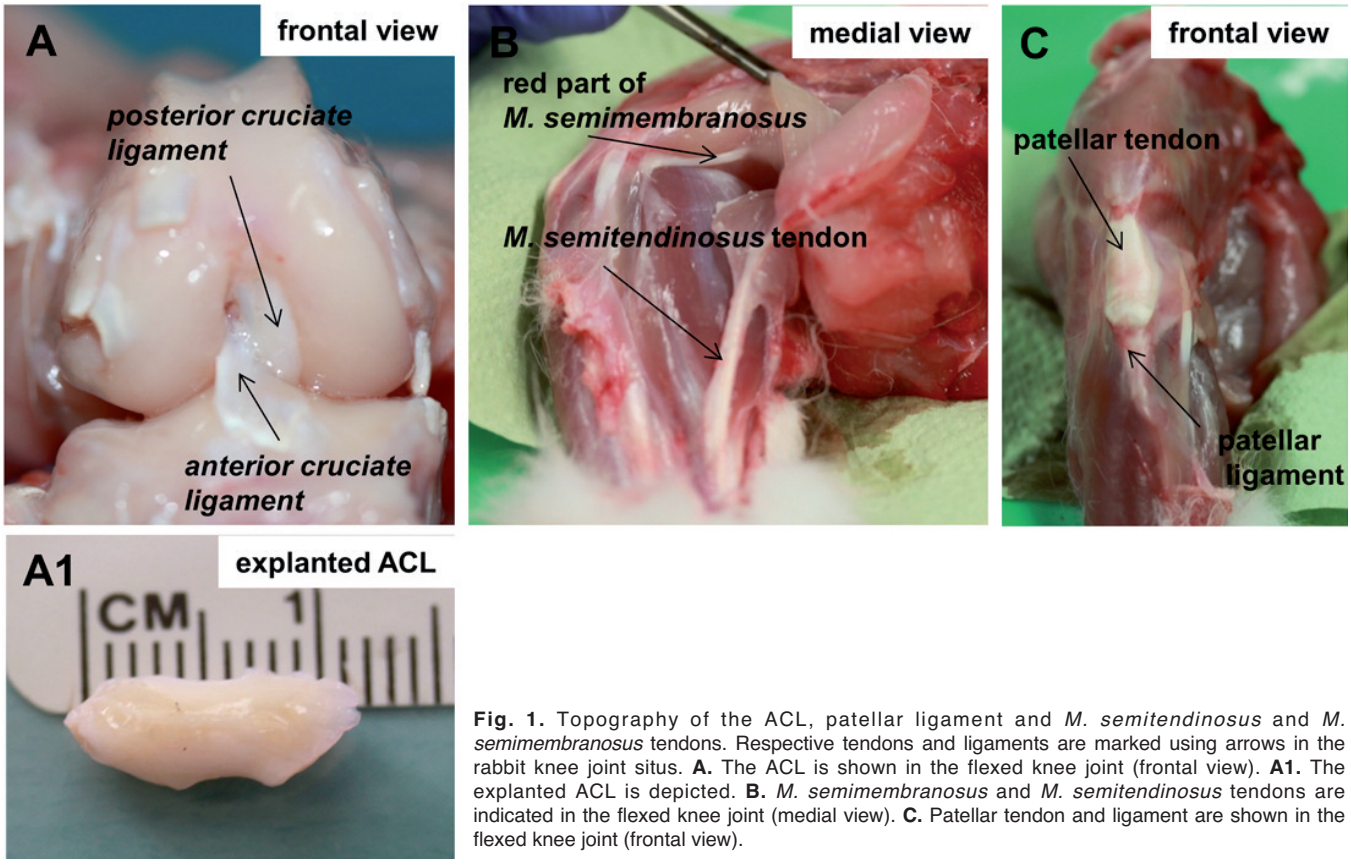

Fig. 1. Topography of the ACL, patellar ligament and *M. semitendinosus* and *M. semimembranosus* tendons. Respective tendons and ligaments are marked using arrows in the rabbit knee joint situs. **A.** The ACL is shown in the flexed knee joint (frontal view). **A1.** The explanted ACL is depicted. **B.** *M. semimembranosus* and *M. semitendinosus* tendons are indicated in the flexed knee joint (medial view). **C.** Patellar tendon and ligament are shown in the flexed knee joint (frontal view).

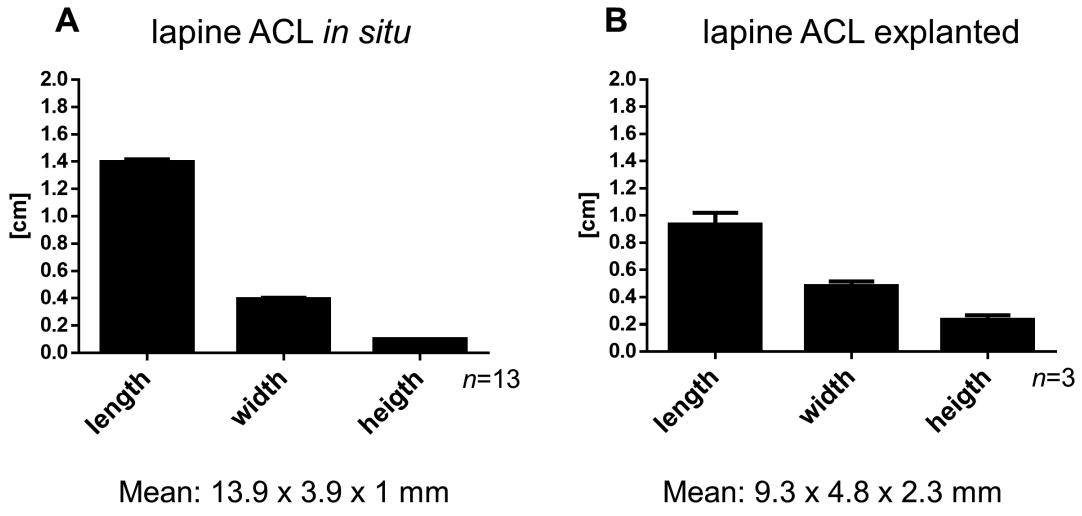

Fig. 2. Macroscopical dimensions of the ACL *in situ* and dimensions of explanted ACLs. **A.** The dimensions of 13 ACLs (derived from adult male New Zealand white rabbits, 2.8-3.5 kg body weight) were measured *in situ* using a caliper. **B.** The dimensions of three of the ACLs were measured after explantation.

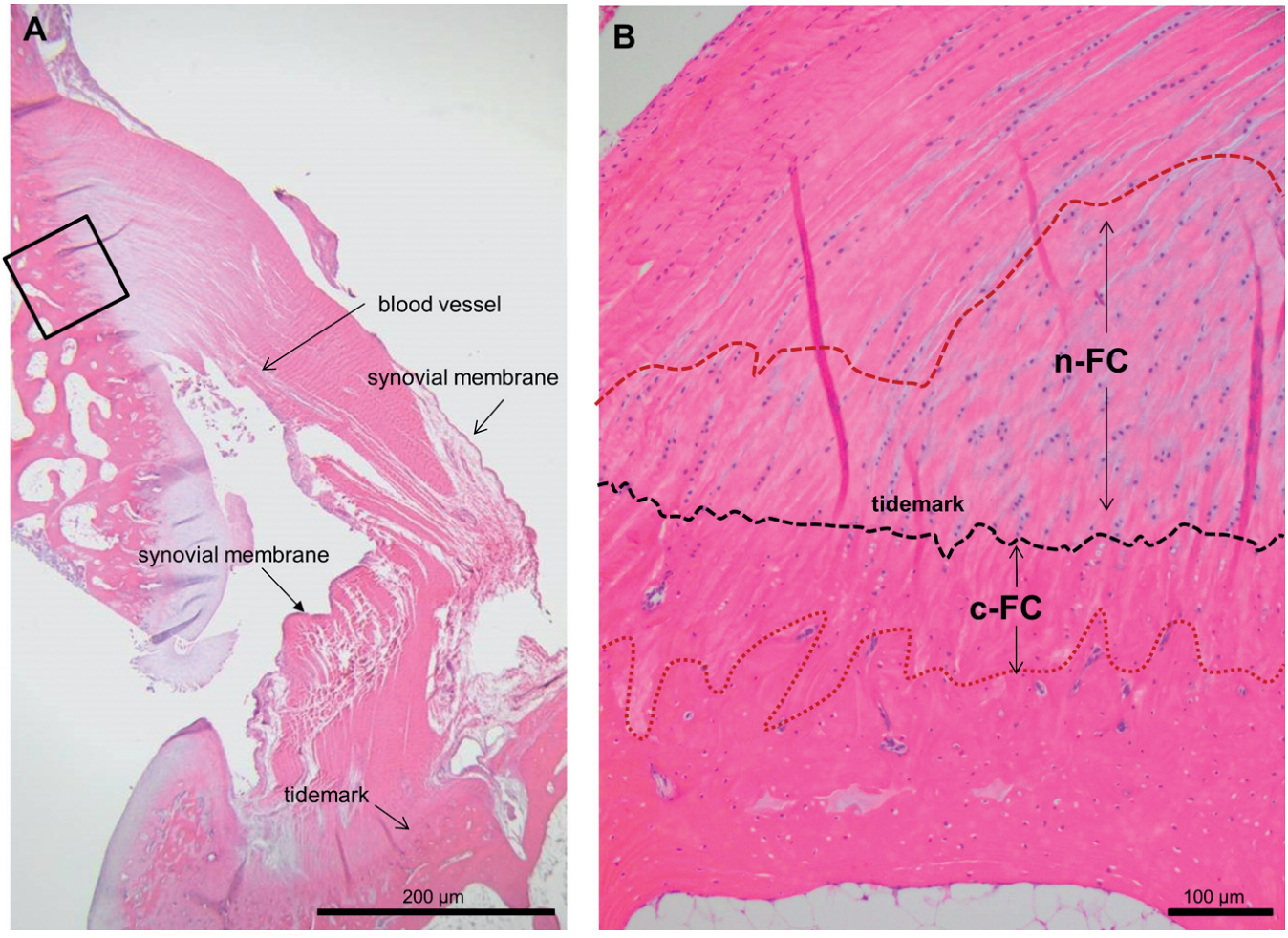

Fig. 3. Histological architecture of the rabbit ACL and its fibrocartilaginous enthesis with zonal dimensions. The fibrocartilaginous enthesis type consists of two zones, which were highlighted in the HE staining: the non-calcified fibrocartilage (n-FC) and the calcified fibrocartilage (c-FC). Both enthesis zones were separated by the tidemark. **A.** Overview. **B.** Detailed view on enthesis region with highlighted zones.

red part of *M. semimembranosus* (origin is the ischial tuberosity) was used instead of *M. semimembranosus* tendon for analysis due to its slim tendon which has similar dimensions to the ACL. Its tendon was attached to the medial femur condyle.

Macroscopical dimension of the lapine ACL

The macroscopical dimensions of the ACL *in situ* were: 13.9x3.9x1 mm. After explantation the size of the ACL was 9.3x4.8x2.3 mm due to elastic properties and subsequent contraction (Fig. 2A,B). The enthesis of the lapine ACL presented a wavy border to the ligament zone and an interdigitating connection to the subligamentous bone as depicted in Fig. 3.

Histological structure of the ACL

The HE staining presented distinct differences in the histological architecture of all analyzed tendons and ligaments. ECM was abundantly present in all investigated tendons and ligaments. Blood vessels were barely detectable. A crimpier ECM fiber bundle pattern was detected in the *M. semimembranosus* and ACL and to a lesser degree in the *M. semitendinosus* tendons compared to the patellar ligament (Fig. 4A-H).

AB and SO stainings visualized sGAGs as components of typical proteoglycans. Both stains

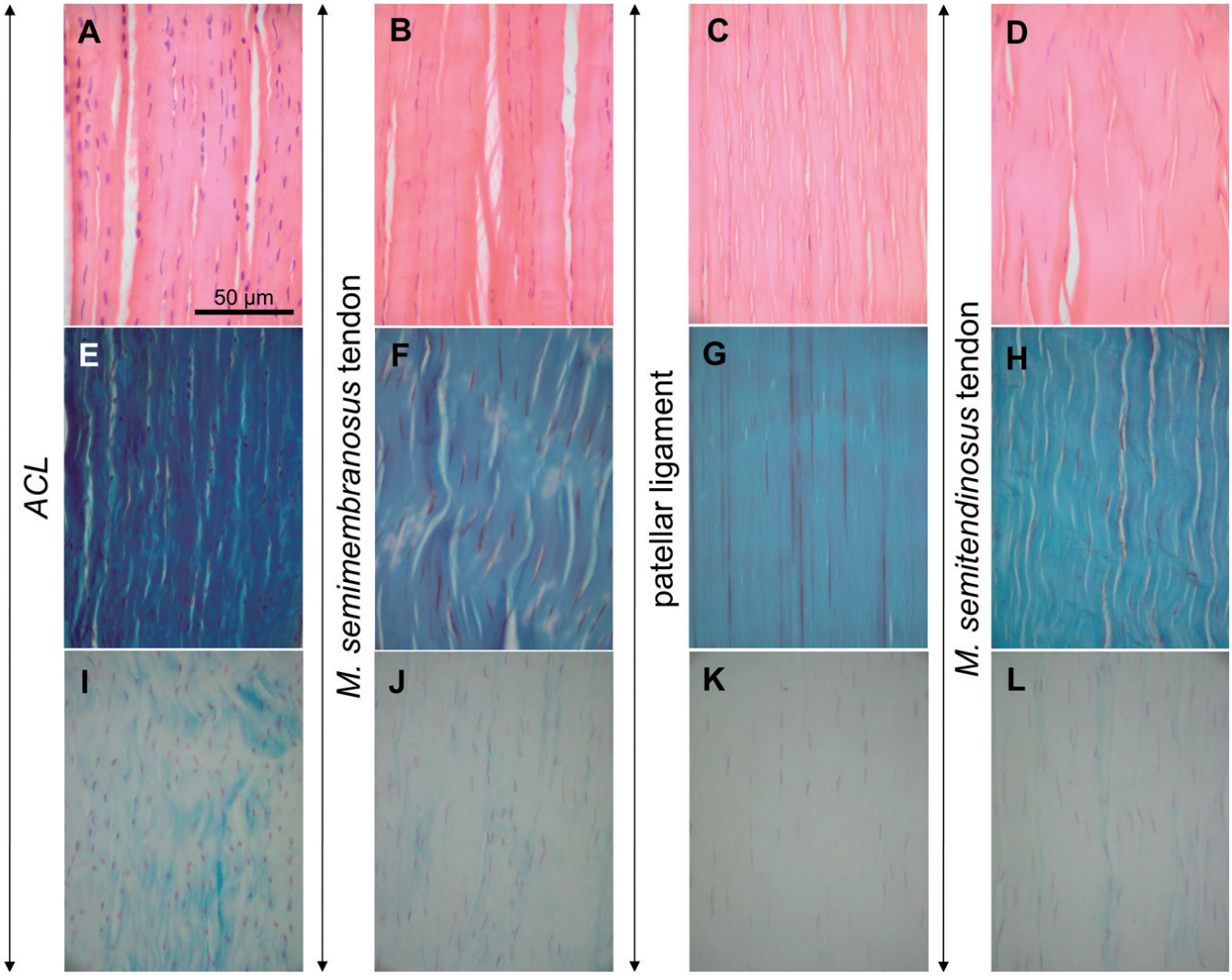

Fig. 4. Histological architecture of rabbit knee joint-associated tendons. Representative images of Hematoxylin Eosin (HE, **A-D)**, Safranin O (SO, **E-H**) and Alcian blue (AB, **I-L)** stainings. SO staining indicates sulfated glycosaminoglycans and cell nuclei in faint red. AB staining shows the cell nuclei in red and the sGAGs in faint blue. **A, E, I.** ACL. **B, F, J.** *M. semimembranosus* tendon. **C, G, K.** Patellar ligament. **D, H, L.** *M. semitendinosus* tendon. Representative images of four (ACL) or three (*M. semimembranosus* tendons, patellar ligaments and *M. semitendinosus* tendons) animals analyzed for each tendon/ligament are shown.

revealed a higher proteoglycan content in the lapine ACL tissue samples compared with the other tendons (Fig. 4E-L).

The use of resorcin-fuchsin staining allowed the detection of a higher content of elastic fibers in the lapine *M. semimembranosus* tendons and ACL ligament compared to the other investigated tissues. The lapine ACLs revealed long elastic fibers whereas in the *M. semimembranosus* tendons they were shorter and often branched (data not shown). The number of blood capillaries was very low in all investigated ligaments and tendons compared to other connective tissues (data not shown).

Cell numbers and dimensions of cell nuclei in various lapine tendons

Cells were distributed in small grouped rows. The cell nuclei number, size and shape differed substantially. The cell number in the lapine ACL was higher than in other tendons, followed by the *M. semimembranosus* tendon (Fig. 5A). A large subgroup of cell nuclei of the ACL were rounded whereas a larger fraction of cell nuclei in the other tendon and ligaments, particularly in the *M. semitendinosus* tendon was elongated (Fig. 4A-D).

The feret diameter was in tendency higher in the *M. semitendinosus* tendons. The ratio between elongated

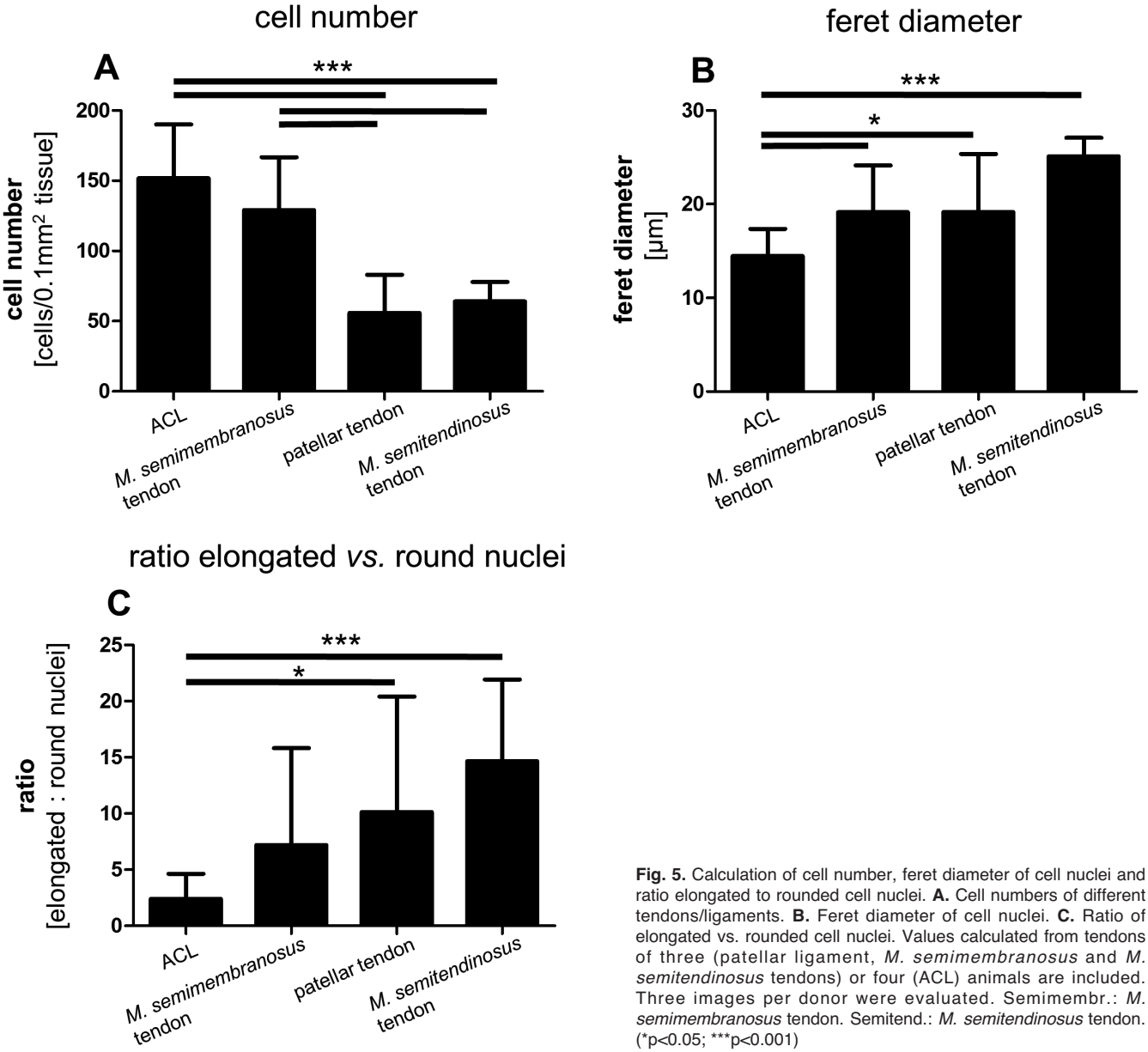

Fig. 5. Calculation of cell number, feret diameter of cell nuclei and ratio elongated to rounded cell nuclei. **A.** Cell numbers of different tendons/ligaments. **B.** Feret diameter of cell nuclei. **C.** Ratio of elongated vs. rounded cell nuclei. Values calculated from tendons of three (patellar ligament, *M. semimembranosus* and *M. semitendinosus* tendons) or four (ACL) animals are included. Three images per donor were evaluated. Semimembr.: *M. semimembranosus* tendon. Semitend.: *M. semitendinosus* tendon. (*p<0.05; ***p<0.001)

and more rounded cell nuclei was higher in the *M. semitendinosus* tendons.

Protein expression in lapine lower extremity derived knee-associated tendons

In regard to the collagen content no significant difference was detected between all analyzed lapine ligaments and tendons but it was not compared with the lapine knee joint cartilage samples since in cartilage another dominating collagen type (type II) was expected. However, the sGAG content was significantly higher in the knee joint cartilage compared with all other analyzed ligaments and tendons except for the lapine ACL. Furthermore, in agreement with the above mentioned sGAG stainings (AB and SO) lapine ACLs had a higher sGAG content compared with the analyzed tendons/ligaments but the quantitative difference was only significant between the ACL and the *M. semitendinosus* tendon (Fig. 6).

Expression of tendon/ligament associated genes in lapine lower extremity derived knee-associated tendons

The mean RNA integrity number (RIN) of all analyzed samples was 7.3 (SD±0.57; MIN 6.3; MAX 8.3). The mean RIN value of human native ACL tissue samples was 8 (SD±0.31).

Lapine *M. semitendinosus* tendons expressed a significantly higher type I collagen level than all other tendons and ligaments analyzed. The human ACL in contrary to the lapine one, expressed significantly lower amounts of decorin mRNA than all investigated tendons. Therefore, the decorin expression level differed substantially between the human and lapine ACLs (Fig. 7). Tenomodulin gene expression was detected in lapine *M. semitendinosus* and *semimembranosus* tendons as well as the patellar ligaments but not in the rabbit ACLs. Additionally, scleraxis and tenascin C expression was shown in human ACLs as fibroblast and tendon markers (data not shown).

Discussion

The anatomical topography of the particular tendons and ligaments included in the present study (*M. semitendinosus*, *M. semimembranosus* and patellar ligaments) differs in the rabbit compared with human conditions. This issue should be considered when using the rabbit as a model for autograft-based ACL reconstruction in humans. The dimensions of the lapine ACLs measured here are in agreement with the data previously reported by other investigators (Hayashi et al., 2008; Hahner et al., 2015). These data are important to design a well-fitting implant in order to plan reconstructive strategies using the rabbit as an animal model.

Until now, comparative approaches to assess differences between rabbit and human ACLs are rare (Amiel et al., 1984; Azangwe et al., 2001; Lo et al., 2004; Kato et al., 2015). The morphological, cell biological and biochemical comparison of the ACL with selected other rabbit derived tendons and ligaments was undertaken to get a guidance level for tissue engineering ACL grafts. The gene and protein expression data reported by us can serve as a quality standard to establish tissue engineered constructs e.g. as reported by Hoyer and Hahner et al. (Hoyer et al., 2014, 2015; Hahner et al., 2015). We restricted the histological analysis to the midsubstance of the tendons, being aware that the dimension and composition of the enthesis parts might also differ between each tendon/ligament. Despite the higher cell content that was detected in the ACL, the nuclear feret diameter was lower compared to the other tendons investigated. Rounded nuclei were distinguished from elongated nuclei in each tendon. One could assume

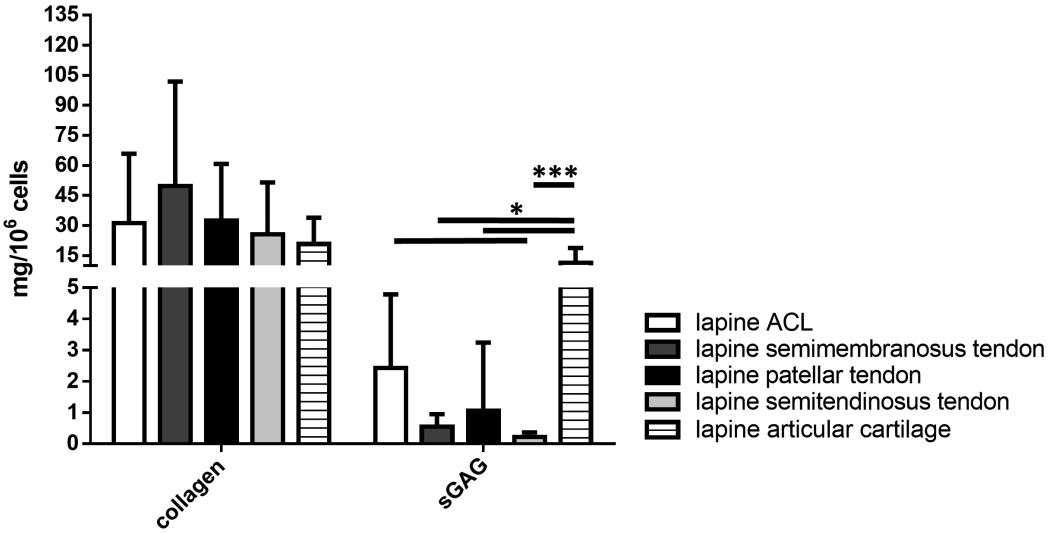

Fig. 6. Total collagen and sGAG content of the ACL, *M. semimembranosus* tendon, patellar ligament and *M. semitendinosus* tendon. Total collagen was determined using hydroxyprolin assay and sGAG content by means of DMMB assay. Values calculated from tendons/ligaments of four (ACL) or three (*M. semimembranosus*, patellar and *M. semitendinosus* tendons/ligaments) animals were included. *p<0.05; ***p<0.001 Lapine ACL, n=5, lapine *M. semitendinosus* tendon, n=10, lapine *M. semimembranosus* tendon, n=12, lapine patellar ligament, n=12, lapine knee joint cartilage, n=5.

a higher metabolic activity for cells with the rounded nuclei. The rounded shape of cells in the ACL is characteristic for ligament fibroblasts, whereas tenocytes usually have elongated cell nuclei (Amiel et al., 1984).

The crimpy structure of the ACL and *M. semimembranosus* tendon tissue could be influenced by the content of the elastic fibers. Elastic fibers were assessed qualitatively by histology using resorcin-fuchsin staining. They could be detected in ACL and *M. semimembranosus* tendon, but to a lesser extend in the *M. semitendinosu*s tendons. This might reflect the local biomechanical microenvironment which differs between particular tendons/ligaments. Also, type I collagen gene expression was higher in *M. semitendinosus* tendons compared with the other tendons and the ACL.

The high proteoglycan content in the ACL confirmed in the present study via the stainings and the DMMB assay probably can be explained by the compressive load resulting from the twisting forces during the natural movement in the knee joint. sGAG content might influence biomechanical properties.

However, the gene expression level of the typical tendon proteoglycan decorin did not show major differences. This in summary suggests that other proteoglycans may also contribute to the net sGAG content.

The biomechanics of the rabbit ACL in direct comparison to tissue engineered constructs has been reported recently (Hahner et al., 2015).

Kato et al. compared the DNA content between ACL and patellar tendon-derived cells cultured until confluence, which did not significantly differ (Kato et al., 2015). When we compared the cell content in both ligaments *in situ* we found more cells in the ACL compared with the patellar ligament. Kato et al. reported a significantly higher expression of tenomodulin in the rabbit patellar tendon- compared with the ACL-derived cells which is in agreement with the present study (Kato et al., 2015). Amiel et al. observed distinct biochemical and morphological differences between tendons and ligaments and smaller variations between particular ligaments (Amiel et al., 1984) when they compared the ACL, the collateral ligaments and the patellar and Achilles tendons of rabbits. They concluded that ligaments are metabolically more active than tendons, possessing more plump cell nuclei, larger amounts of reducible collagen cross-links, and the presence of more type III collagen, when compared with tendons (Amiel et al., 1984). Indeed, we also found more cells with a rounded nuclear shape in the ACL compared to the tendons but not in the patellar ligament. In agreement with the report of Amiel et al., we detected more sGAGs in the ACL compared to the other tendons. Additionally, Amiel et al., observed that ligaments contained slightly less total collagen than tendons (Amiel et al., 1984). This observation could be confirmed by a higher type I collagen gene expression in the *M. semitendinosus* tendon compared to the ACLs in our study without a significant difference in the total collagen content.

If the use of a cell-seeded tissue engineered ACL construct is desired for ACL reconstruction the cell source and the supporting scaffold has to be properly selected. The results suggest that the use of ACL cells might represent the most suitable cell source due to their

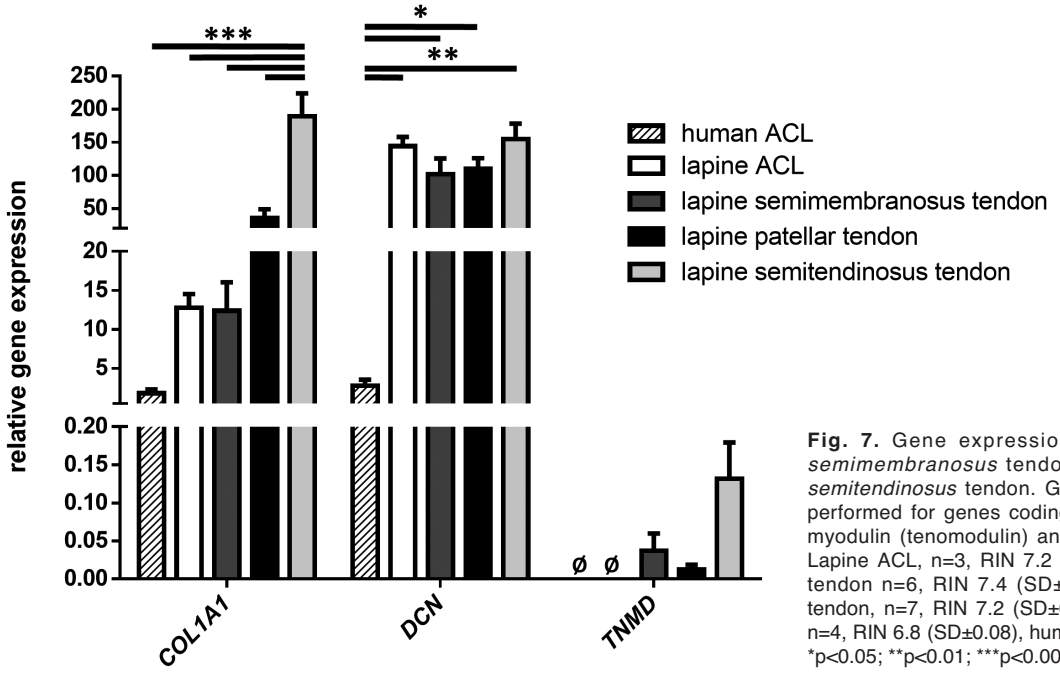

Fig. 7. Gene expression analysis in the ACL, *M. semimembranosus* tendon, patellar ligament and *M. semitendinosus* tendon. Gene expression analysis was performed for genes coding for type I collagen, decorin, myodulin (tenomodulin) and normalized versus GAPDH. Lapine ACL, n=3, RIN 7.2 (SD±0.25), *M. semitendinosus* tendon n=6, RIN 7.4 (SD±0.57), *M. semimembranosus* tendon, n=7, RIN 7.2 (SD±0.58), lapine patellar ligament. n=4, RIN 6.8 (SD±0.08), human ACL, n=3, RIN 8 (SD 0.31). *p<0.05; **p<0.01; ***p<0.001

specific synthetic profile. The question arises whether indeed other tendons or mesenchymal stem cells can be used as a cell source for ligament TE. Despite being promising as a more abundant and proliferative cell source than tenocytes in future, the use of precursor tendon cells such as MSCs requires time for tenogenic differentiation and the induction of stable differentiation is not reliable.

All tendons/ligaments have a special micro-environment. As supported by the data, they show some differences in histoarchitecture and at the biochemical level, although a transdifferentiative shift of tendon tissue in a ligament-like tissue profile has been reported (Amiel et al., 1986; Claes et al., 2011). A remodeling process of *M. semitendinosus* and *semimembranosus* tendons and patellar tendon/ligament autografts after implantation for ACL reconstruction has been observed – called previously "ligamentalization" (Amiel et al., 1986; Blickenstaff et al., 1997; Marumo et al., 2005; Claes et al., 2011). This process requires time but could be observed within one year post-operatively (Marumo et al., 2005). Ligamentalization is a result of the graft's response to its new milieu influenced by the neighbored synovial membrane and new physical forces (Amiel et al., 1986).

Conclusion

In summary, we present in this project the dimensions of the lapine ACL and demonstrated some unique biochemical features which can serve as an orientation for ACL scaffold design for the rabbit ACL reconstruction model. In comparison to other tendons, which are used as autografts for ACL reconstruction, the ACL reveals higher sGAG content and lower type I collagen gene expression. The ACL showed higher cell content than most of the other tendons with cells mostly exhibiting a rounded shape and a lower feret diameter of the nuclei.

Apart from the sGAG content, the lapine ACL shared more similarities with the *M. semimembranosus* tendon compared with the other tendons included in this study regarding the investigated parameters. This might be of importance since the *M. semitendinosus* tendon is usually preferred for reconstructive approaches.

Acknowledgements. The authors are grateful for the support of Drs. Claudia and Barbe Rentsch and Stefan Arens. Furthermore, they would like to thank Marion Lemke for the technical assistance. This study was funded by the German Research Foundation (DFG-SCHU1979/9-1). The authors confirm that this manuscript has not been published previously. It is not under consideration for publication elsewhere, and, if accepted, it will not be published elsewhere in the same form, in English or in any other language. All co-authors approved the manuscript.

References

Amiel D., Frank C., Harwood F., Fronek J. and Akeson W. (1984). Tendons and ligaments: a morphological and biochemical comparison. J. Orthop. Res. 1, 257-265.

Amiel D., Kleiner J.B., Roux R.D., Harwood F.L. and Akeson W.H. (1986). The phenomenon of "ligamentization": anterior cruciate ligament reconstruction with autogenous patellar tendon. J. Orthop. Res. 4, 162-172.

Arnoczky S.P. (1985). Blood supply to the anterior cruciate ligament and supporting structures. Orthop. Clin. North Am. 16, 15-28.

Azangwe G., Mathias K.J. and Marshall D. (2001). Preliminary comparison of the rupture of human and rabbit anterior cruciate ligaments. Clin. Biomech. (Bristol, Avon). 16, 913-917.

Bachy M., Sherifi I., Zadegan F., Petrover D., Petite H. and Hannouche D. (2013). Anterior cruciate ligament surgery in the rabbit. J. Orthop. Surg. Res. 8, 27.

Benedetto K.P. and Klima G. (1986). Effect of the Hoffa fat pad on revascularization of the ruptured anterior cruciate ligament. A histologic study of the rabbit model. Z. Orthop. Ihre Grenzgeb. 124, 262-265. (in German).

Biscarini A., Botti F.M. and Pettorossi V.E. (2013). Selective contribution of each hamstring muscle to anterior cruciate ligament protection and tibiofemoral joint stability in leg-extension exercise: a simulation study. Eur. J. Appl. Physiol. 113, 2263-2273.

Blickenstaff K.R., Grana W.A. and Egle D. (1997). Analysis of a semitendinosus autograft in a rabbit model. Am. J. Sports Med. 25, 554-559.

Chambat P. (2013). ACL tear. Orthop. Traumatol. Surg. Res. 99 (1 Suppl), S43-52.

Claes S., Verdonk P., Forsyth R. and Bellemans J. (2011). The "ligamentization" process in anterior cruciate ligament reconstruction: what happens to the human graft? A systematic review of the literature. Am. J. Sports Med. 39, 2476-2483.

Eriksson K., Hamberg P., Jansson E., Larsson H., Shalabi A. and Wredmark T. (2001). Semitendinosus muscle in anterior cruciate ligament surgery: Morphology and function. Arthroscopy 17, 808-817.

Fenwick S.A., Hazleman B.L. and Riley G.P. (2002). The vasculature and its role in the damaged and healing tendon. Arthritis Res. 4, 252-260.

Hahner J., Hinüber C., Breier A., Siebert T., Brünig H. and Heinrich G. (2015). Adjusting the mechanical behavior of embroidered scaffolds to lapin anterior cruciate ligaments by varying the thread materials. Textile Res. J. 85, 1434-1444.

Hayashi, R., Kondo, E., Tohyama, H., Saito, T. and Yasuda, K. (2008). In vivo local administration of osteogenic protein-1 increases structural properties of the overstretched anterior cruciate ligament with partial midsubstance laceration: a biomechanical study in rabbits. J. Bone Joint Surg. Br. 90, 1392-1400.

Homicz M R., McGowan K.B., Lottman L.M., Beh G., Sah R.L. and Watson D. (2003). A compositional analysis of human nasal septal cartilage. Arch. Facial Plast. Surg. 5, 53-58.

Hoyer M., Drechsel N., Meyer M., Meier C., Hinuber C., Breier A., Hahner J., Heinrich G., Rentsch C., Garbe L.A., Ertel W., Schulze-Tanzil G. and Lohan A. (2014). Embroidered polymer-collagen hybrid scaffold variants for ligament tissue engineering. Mater Sci. Eng. C Mater. Biol. Appl. 43, 290-299.

Hoyer M., Meier C., Breier A., Hahner J., Heinrich G., Drechsel N., Meyer M., Rentsch C., Garbe L.A., Ertel W., Lohan A. and Schulze-Tanzil G. (2015). In vitro characterization of self-assembled anterior cruciate ligament cell spheroids for ligament tissue engineering. Histochem. Cell Biol. 143, 289-300.

Kato S., Saito M., Funasaki H. and Marumo K. (2015). Distinctive

collagen maturation process in fibroblasts derived from rabbit anterior cruciate ligament, medial collateral ligament, and patellar tendon in vitro. Knee Surg. Sports Traumatol Arthrosc. 23, 1284-1392.

Kawai T., Yamada T., Yasukawa A., Koyama Y., Muneta T. and Takakuda K. (2010). Anterior cruciate ligament reconstruction using chitin-coated fabrics in a rabbit model. Artif. Organs. 34, 55-64.

Lee A.J., Chung W.H., Kim D.H., Lee K.P., Chung D.J., Do S.H. and Kim H.Y. (2012). Anterior cruciate ligament reconstruction in a rabbit model using canine small intestinal submucosa and autologous platelet-rich plasma. J. Surg. Res. 178, 206-215.

Livak K.J. and Schmittgen T.D. (2001). Analysis of relative gene expression data using real-time quantitative PCR and the 2(-Delta Delta C(T)) method. Methods 25, 402-408.

Lo I.K., Marchuk L.L., Leatherbarrow K.E., Frank C.B. and Hart D.A. (2004). Collagen fibrillogenesis and mRNA levels in the maturing rabbit medial collateral ligament and patellar tendon. Connect. Tissue Res. 45, 11-22.

Marumo K., Saito M., Yamagishi T. and Fujii K. (2005). The "ligamentization" process in human anterior cruciate ligament reconstruction with autogenous patellar and hamstring tendons: a biochemical study. Am. J. Sports Med. 33, 1166-1173.

Petrigliano F.A., McAllister D.R. and Wu B.M. (2006). Tissue engineering for anterior cruciate ligament reconstruction: a review of current strategies. Arthroscopy 22, 441-451.

Shen W., Chen X., Hu Y., Yi Z., Zhu T., Hu J., Chen J., Zheng Z., Zhang W., Ran J., Heng B.C., J, J., Chen W. and Ouyang H.W. (2014). Long-term effects of knitted silk-collagen sponge scaffold on anterior cruciate ligament reconstruction and osteoarthritis prevention. Biomaterials 35, 8154-8163.

Tohyama H., Yoshikawa T., Ju Y.J. and Yasuda K. (2009). Revascularization in the tendon graft following anterior cruciate ligament reconstruction of the knee: its mechanisms and regulation. Chang Gung Med. J. 32, 133-139.

Accepted January 21, 2016